IOP Publishing Journal of Physics: Condensed Matter
J. Phys.: Condens. Matter **32** (2020) 205504 (7pp) https://doi.org/10.1088/1361-648X/ab6e90

Theoretical study on the effect of the optical properties and electronic structure for the Bi-doped $CsPbBr_3$

Zhuo-Liang Yu[1], Yu-Qing Zhao[2], Qiang Wan[1,4], Biao Liu[3], Jun-Liang Yang[3,4] and Meng-Qiu Cai[1,4]

[1] Key Laboratory for Micro/Nano Optoelectronic Devices of Ministry of Education and Hunan Provincial Key Laboratory of Low-Dimensional Structural Physics and Devices, School of Physics and Electronics, Hunan University, Changsha 410082, People's Republic of China
[2] School of Physics and Electronic Science, Hunan University of Science and Technology, Xiangtan 411201, People's Republic of China
[3] Hunan Key Laboratory for Super-microstructure and Ultrafast Process, School of Physics and Electronics, Central South University, Changsha 410083, Hunan, People's Republic of China

E-mail: mqcai@hnu.edu.cn, wanqiang@hnu.edu.cn and junliang.yang@csu.edu.cn

Received 28 October 2019, revised 29 December 2019
Accepted for publication 22 January 2020
Published 20 February 2020

Abstract

Metal doping, including Bi, Yb, Eu, Sb and so on, are important means to improve the photoelectric properties and stability of metal halide perovskite materials. Among these works, Bi-doped $CsPbBr_3$ especially has attracted much attention for both experimental and theoretical investigation. But there are still some arguments to be solved. One view thinks that Bi doping in $CsPbBr_3$ not only influences the band structure, but also improves the charge transfer (Raihana *et al* 2017 *J. Am. Chem. Soc.* **139** 731–7). The other supported the points that there are no changes in the valence band structure of Bi-doped $CsPbBr_3$ and the concept of the band-gap engineering in Bi-doped $CsPbBr_3$ halide perovskite is not valid (Olga *et al* 2018 *J. Phys. Chem. Lett.* **9** 5408–11). They also have different opinions for the reason of the red-shift phenomenon caused by Bi-doped $CsPbBr_3$. In this work, the density functional theory (DFT) based first-principles methods is adopted to investigate the effect of the optical properties and electronic structure for Bi doping $CsPbBr_3$. The calculated results clarify that the red-shift phenomenon is caused by the slight reduction of band gap and the transition levels of Bi_i and Bi_{Pb} defects. The values of red-shift also were estimated about 150 meV for Bi_i defects, which is close the experimental value of about 140 meV. Moreover, our studies also show that the Bi doping does not affect the valence bands, but Bi_i defects change the electron distribution of the conduction band. Our work and experimental results support and confirm each other, which provides a useful reference for the study of Sb-doped $CsPbBr_3$, Eu-doped $CsPbBr_3$ and so on.

Keywords: metal halide perovskite, photoelectric properties, red-shift phenomenon, electron distribution

(Some figures may appear in colour only in the online journal)

[4] Author to whom any correspondence should be addressed.

1. Introduction

Owing to the excellent electronic and optical properties coupled with low cost, the halide perovskites have attracted great attention of researchers. In recent years, using metal halide perovskite, researchers have made great progress in the field of solar cells and light-emitting devices. Zhiping Wang *et al* create the current record of photoelectric conversion efficiency, 23.6% [1]. The external quantum efficiency (EQE) of perovskite light-emitting diodes exceeds 20%, which also sets the world record for perovskite light-emitting diodes [2, 3]. In the study of metal halide perovskite, metal doping is one of the important means to adjust the photoelectric properties and improve the stability of perovskite. For example, Zhang *et al* observed that Sb-Doped $CsPbBr_3$ show strong blue emission [4]. Hu *et al* found that doping Eu can strengthen the competitiveness of lighting application based on $CsPbBr_3$ [5]. And Anu *et al* thought that doping Eu also improves the stability of $CsPbBr_3$ according to the density functional theory (DFT)-based first-principles methods [6]. Yang *et al* concluded that the different metal doping has different effects [7]. The doping of K, Rb, Mn and Bi is beneficial to the stabilization of perovskite structure. The doping of Li, Na and Bi is beneficial to the regulation of photoelectric properties [7]. Because the valence electronic shell is isoelectronic to lead and the ns^2 lone pair is essential for defect tolerance, the Bi-doped metal halide perovskite has become a research hotspot in the past year [8, 9]. Raihana *et al* concluded that Bi doping in $CsPbBr_3$ not only influences the band structure, but also improves the charge transfer [8]. However, Olga *et al* demonstrates that the concept of the band-gap engineering in Bi-doped $CsPbBr_3$ halide perovskite is not valid [9]. Their results show that no changes in the valence band structure of $CsPbBr_3$ with the doping of Bi [9]. They attributed the apparent red-shift caused by Bi doping to the defect states caused by Bi impurities [9]. The different opinions of Raihana and Olga also blur the cause of red-shift in the spectra caused by Bi doping. Now there are three urgent problems to be solved. What defects are induced by Bi doping? What is the cause of red-shift? Will Bi impurities cause changes in band structure of $CsPbBr_3$? However, there is no theoretical study on Bi-doped $CsPbBr_3$. It is necessary to analyze Bi-doped $CsPbBr_3$ from theories.

In this paper, we studied the formation energy of defects caused by Bi impurities and the transition level of these defects by the DFT-based first-principles methods. The results show that the defect of Bi_{Pb} (Bi atoms replaces Pb atoms) and Bi_i (Bi atoms in the interstices) are more stable. And the formation energy of Bi_{Cs} (Bi atoms replaces Cs atoms) defect is lager than that of Bi_{Pb} and Bi_i defects, so the Bi_{Cs} defect is not stable as the Bi_{Pb} and Bi_i defects. Further studies show that the transition energy levels of the Bi_{Pb} and Bi_i defects are close to the conduction band of $CsPbBr_3$, which indeed cause red-shift phenomenon. Moreover, the influence of different defects on the electronic structure of $CsPbBr_3$ is also discussed. Due to the addition of Bi atom, the crystal lattice of $CsPbBr_3$ changed slightly, resulting in a about 0.1 eV reduction in band gap. Bi atoms did not change the valence band as the conclusion of Olga *et al*, but the Bi_i defect affected the density of states near the conduction band. This work determined that Bi_i and Bi_{Pb} defects are stable, explained the mechanism of red-shift phenomenon, estimated the value of red-shift caused by Bi_i and Bi_{Pb} defects (150 meV and 270 meV close the experimental value, 140 meV) and explored the effect of Bi doping on charge distribution. Our work and experimental results support and confirm each other, which not only theoretically analyses and explains experiments, but also provides a useful reference for the study of Sb-doped $CsPbBr_3$, Eu-doped $CsPbBr_3$ and so on.

2. Computational methods

DFT calculations were carried out using the Vienna *ab initio* simulation package (VASP) in this paper [10, 11]. The core-valence interaction was described by the projected augmented wave (PAW) method. The calculations were both employed by the generalized gradient approximation (GGA) of Perdew–Burke–Ernzerh (PBE) exchange-correlation functional and the Heyd–Scuseria–Ernzerhof hybrid functional (HSE06) method [12–52]. The spin-orbit coupling (SOC) effect was included in calculations [12–14]. In our calculations, $3 \times 3 \times 3$ super cell were used. Because of the large lattice of the super cell, the volume of *K*-spacing is small. We adopt point-only *k*-mesh for defect calculations [53]. All atoms are fully relaxed until the atomic Hellmann–Feynman forces are smaller than 0.02 eV $Å^{-1}$ and the convergence criterion of energy in the self-consistency process is set to 10^{-4} eV. The energy cutoff is set as 350 eV. For a defect with a charge state q, the formation energies ΔH is calculated through the equation [54, 55]:

$$\Delta H(\alpha, q) = E(\alpha, q) - E^{p}_{tot} - n_i(\mu_i^{bulk} + \Delta\mu_i) + q(E_{VBM} + E_f + \Delta V) \quad (1)$$

where $(E(\alpha, q) - E^{p}_{tot})$ is the energy difference between the total energy of defect system and perfect system with out defect. n_i is the number of impurities. $\Delta\mu_i$ is the chemical potential of impurity atoms relative to that of bulk (μ_i^{bulk}). And E_f represents the Fermi level relative to the valence band maximum (VBM) of perfect $CsPbBr_3$ bulk. Thus E_{VBM} is always set to zero. $q\Delta V$ included the potential alignment correction term and image-charge correction term [56]. Calculating the density of states (DOS), $5 \times 5 \times 5$ *k*-mesh was used.

3. Results and discussion

Figures 1(a)–(d) show four systems: no doping, Bi atoms substituting Cs atoms (Bi_{Cs}), Bi atoms substituting Pb atoms (Bi_{Pb}), Bi atoms in the interstices of $CsPbBr_3$ (Bi_i). In this paper, we did not consider the condition of Bi atoms replacing I atoms. When cations replace anions, cations repel each other, resulting in an increase in the formation energy of the Bi impurities. Previous studies have also shown that the formation of such defects (cation-on-anion antisites or anion on-cation antisites) is large [12, 55]. In the next section, we will carefully analyze the formation energy of these three defects.

The PBE method and the HSE06+SOC method were used to calculate the energy of these systems respectively. In the table 1, the system energies calculated by the two methods

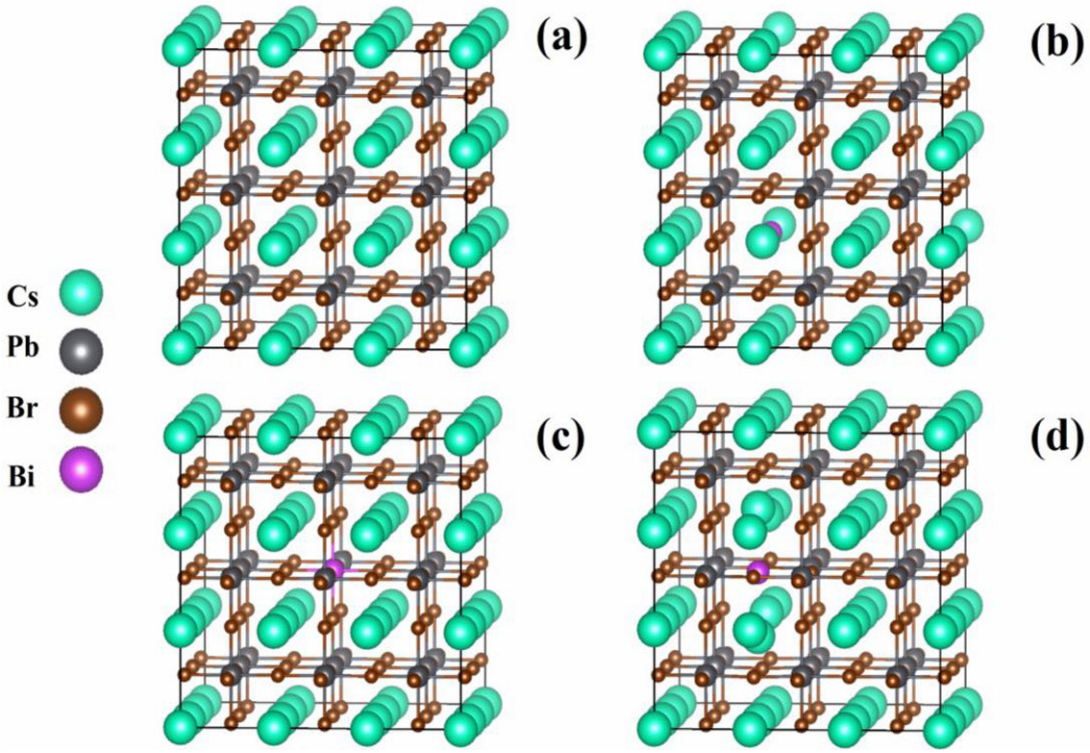

Figure 1. Model schematic diagrams for calculations. (a) Perfect $CsPbBr_3$ without Bi-doping. (b) $CsPbBr_3$ with Bi_{Cs} defects. (c) $CsPbBr_3$ with Bi_{Pb} defects. (d) $CsPbBr_3$ with Bi_i defects.

Table 1. The total energy of four systems (no doping, Bi_{Cs}, Bi_{Pb} and Bi_i) at different charge states. The PBE method and HES06+SOC method are used for these data.

Method	PBE				HSE06+SOC			
Charge State	0	+1	+2	+3	0	+1	+2	+3
No doping	−431.73	—	—	—	−529.43	—	—	—
Bi_{Cs}	−428.82	−429.83	−430.71	—	−529.58	−529.24	−528.84	—
Bi_{Pb}	−429.98	−432.83	—	—	−528.81	−530.80	—	—
Bi_i	−432.77	−435.43	−436.71	−436.91	−532.55	−535.06	−535.88	−535.68

are compared. As we all know, the PBE calculation method will lead to a larger energy value of the system, because this method will increase self-interaction error [19]. The HSE06+SOC methods could overcome this error in the PBE calculation. However, because the Bi atoms and Pb atoms contain a large number of *d*-orbital electrons, the occupancy of d-orbital is reduced too much when using HSE06+SOC method [57]. Therefore, the energy of the system will be greatly reduced. The result calculated by one method alone can not accurately determine the defect formation energy. In order to make a more accurate judgment, we will consider the results calculated by the two methods.

As shown in the figures 2(a) and (b), the formation energy ΔH calculated by the two methods can be compared. The abscissa of the orange dotted line in the figure is 2.36 eV, which represents the conduction band minimum (CBM) of $CsPbBr_3$. Obviously, the formation energy obtained by the PBE method is greater than that of the HSE06+SOC method as shown in the table 1. As shown in the figure 2(a), the formation energy of the defect Bi_{Cs} is the largest, that of the defect Bi_i is the second, and that of the defect Bi_{Pb} is the smallest. As shown in the figure 2(b), the formation energy of the defect Bi_{Cs} is still the largest. However, the formation energy of the defect Bi_{Pb} is larger than that of the defect Bi_i. The calculation results obtained by two methods both show that the defect Bi_{Cs} is unstable due to excessive formation energy. According to the previous discussion, the actual value of formation energy of the defect Bi_{Pb} and Bi_i should lie between the two results obtained by two methods. Therefore, the formation of these two defects are very close, suggesting that the defects Bi_{Pb} and Bi_i may both occur in $CsPbBr_3$ crystals. We further analyzed the reasons. As we all know, there is a strong correlation between the stability of halide perovskite and tolerance factors *t*. *t* is calculated through the equation [58]:

$$t = (R_A + R_x)/\{\sqrt{2}(R_B + R_x)\}. \quad (2)$$

Where the value of R_A, R_B, and R_X is the ionic radii of Cs, Pb and Br in the $CsPbBr_3$. When t close to 1, the perovskite structure is more stable. The ionic radius of Cs, Pb and Bi are 1.74 Å, 1.19 Å and 1.03 Å respectively. When Bi atoms replaces Cs

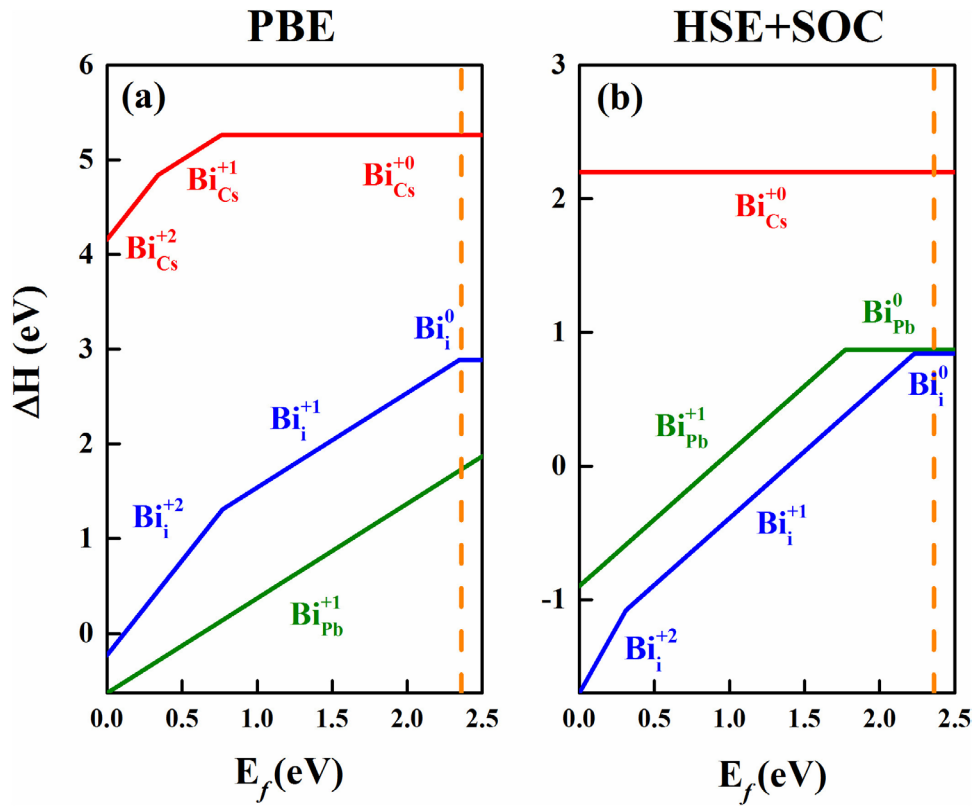

Figure 2. The functional relationship between the Fermi level and the formation energy of Bi_{Cs}, Bi_{Pb} and Bi_i defects. (a) The data are calculated by the PBE method. (b) The data are calculated by the HSE +SOC method. The energy level of the VBM is set to zero. The dotted line represents the location of CBM.

atoms, t tends to decrease, which is not beneficial for the stability of the structure. Therefore, the formation energy of Bi_{Cs} defects is large. Due to the ion radius of Bi being slightly smaller than that of Pb, Bi atoms substitution for Pb atoms does not cause a significant change in t. Thus the defect Bi_{Pb} is more stable than the defect Bi_{Cs}. The distance between adjacent nearest Pb atoms in the $CsPbBr_3$ is 5.96 Å, much larger than ion radius of Bi. It implies that the interstices in $CsPbBr_3$ can accommodate Bi ions. Moreover, the symmetrical distribution of Pb and I ions around Bi ions counteracts the strong Coulomb interaction, which makes the Bi_i defects stable.

Based on the above discussion on the formation energy of defects, we have determined that the defects induced by Bi doping in the $CsPbBr_3$ are Bi_i and Bi_{Pb}, respectively. In this section, we would discuss whether defect-induced transition levels can cause red shift in light absorption.

The figure 3 shows the transition levels of defects Bi_i and Bi_{Pb} in $CsPbBr_3$. The transition level of an impurity, $\varepsilon(q, q')$, is given by [54, 55]:

$$\varepsilon(q, q') = \frac{\Delta H(\alpha, q) - \Delta H(\alpha, q')}{q' - q}. \quad (3)$$

The equation (3) denoted that the abscissas of inflection points of curves in figure 2 correspond to the energy value of transition level shown in the figure 3. Obviously, the energy of transition level obtained by PBE method is higher than that obtained by HSE06+SOC method because of the over-consideration of self-interaction in PBE method and the over-reduction of d-orbital energy in HSE06+SOC method. With this in mind, the true energy value of transition levels are expected to be located between the energy values calculated by the PBE and HSE06+SOC methods. Therefore, we took the average values calculated by PBE method and HSE06+SOC method as the real energy values of transition energy levels. In addition to the (+2/+ 3) transition level of Bi_i as a shallow donor level, the (0/+ 1) transition level of Bi_i, the (+1/+2) transition level of Bi_i and the (0/+1) transition level of Bi_{pb} are deep donor levels. It should be noted that there are still errors between the transition level (by taking the average values) and the real transition level. The closer the transition level calculated by PBE and HSE +SOC method is, the more accurate the position of transition level is. For example, the calculated (0/+1) transition level of Bi_i is the most accurate in our paper. Because the energy values of (0/+1) Bi_i transition level calculated by the PBE and HSE06+SOC methods are only about 0.1 eV different. It is suggested that the energy difference between the real (0/+1) Bi_i transition level and the estimated (0/+1) Bi_i transition level is about ±0.05 eV. And the error of other calculated transition levels would be slightly larger. Using ultraviolet photoelectron spectroscopy (UPS) measurements, Olga *et al* observed an increase in the Fermi level by 0.6 eV [9]. As we all know, the band gap of $CsPbBr_3$ without any impurities is 2.36 eV. The Fermi energy of $CsPbBr_3$ without any impurity is close to the middle of the forbidden band, 1.18 eV (the VBM of perfect $CsPbBr_3$ is set to zero). Thus the Fermi energy of $CsPbBr_3$ with Bi impurities is about 1.78 eV close to the

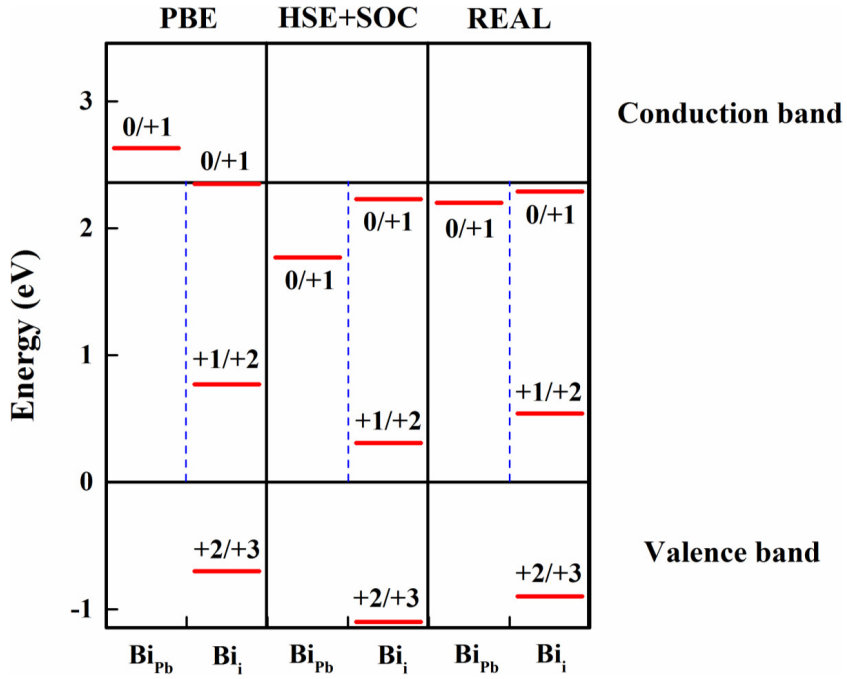

Figure 3. The charge-state transition level for Bi_{Cs}, Bi_{Pb} and Bi_i defects. The data are calculated by the PBE method and HSE06 +SOC method. The average energy values calculated by PBE method and HSE06 +SOC method are approximated as the real transition energy levels.

CBM of $CsPbBr_3$. Combined with the figure 2, when Fermi level is close to CBM, the defects Bi_i and Bi_{Pb} is more likely to exhibit +1 charge state or neutral state. Under this condition, the (0/+1) transition levels of Bi_i and Bi_{pb} are easier to form. According to the calculation, the corresponding energy value of (0/+1) transition levels of Bi_i and Bi_{pb} are 2.29 eV and 2.2 eV. Clearly, the (0/+1) transition levels of Bi_i and Bi_{pb} are very close to CBM (2.36 eV). As donor levels, the two transition levels can bind the electrons excited by the valence band. Because the transition level is lower than CBM, the electrons can be excited with absorbing <2.36 eV energy, which eventually leads to the red shift of the absorption spectrum. The red shift caused by the transition level is the difference between the energy of transition level and CBM, 0.07 eV and 0.16 eV. The Bi_i and Bi_{pb} also cause small changes in $CsPbBr_3$ lattice, resulting in the decrease of band gaps of 0.08 and 0.11 eV (This will be discussed in more detail later.) Therefore, the total red shifts are 150 meV and 270 meV, which are in good agreement with the experimental red shifts of 140 meV [9]. It also shows that the judgement about defect type in above discussion is correct. It is noteworthy that the red shift caused by transition levels can not improve the excitation efficiency of electrons. As mentioned earlier, electrons are excited but bound by these transition levels. When these bound electrons recombine with holes from the conduction band, no photon are excited, but quenched in a non-radiative manner. A large number of defects will lead to the decrease of device efficiency. The red shift caused by transition levels is essentially different from the red shift caused by the reduction of band gap.

The effect of defects on the electronic structure of $CsPbBr_3$ is discussed in the last section. As show in the figure 4, we

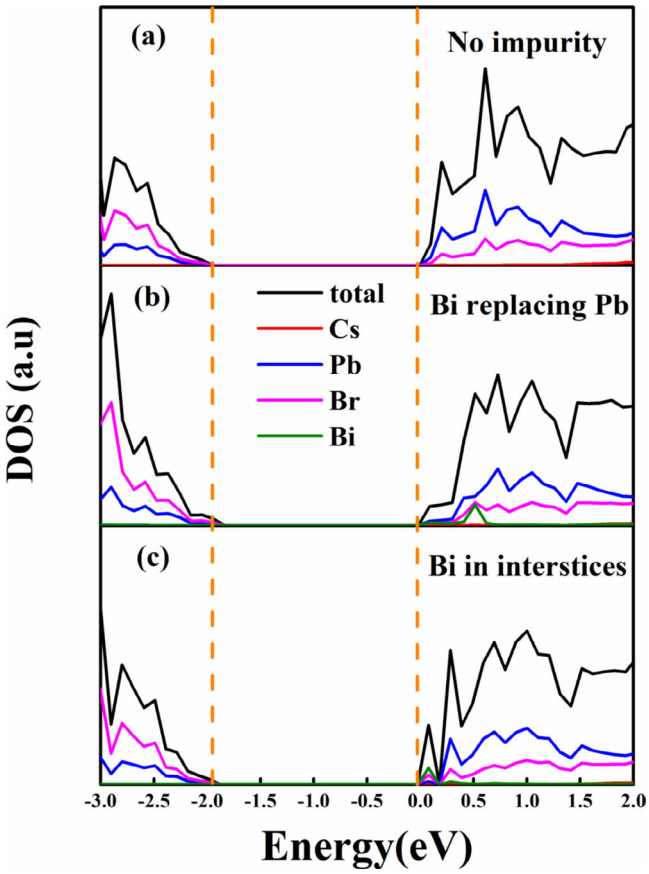

Figure 4. The density-of-states (dos) diagram of three different systems. (a) Perfect $CsPbBr_3$ without Bi-doping. (b) $CsPbBr_3$ with Bi_{Pb} defects. (c) $CsPbBr_3$ with Bi_i defects.

compared the density of states in three different conditions, including the perfect $CsPbBr_3$, the $CsPbBr_3$ with Bi_{Pb} defects and the $CsPbBr_3$ with Bi_i defects. Bi_{Pb} defects and Bi_i defects cause a weak decrease in band gap, which is 0.08 eV and 0.11 eV, respectively. Whatever the case, we also clearly observe that the states on the valence band are supplied by Br atoms. This conclusion is in agreement with the experiment of Olga *et al* [9]. They concluded that no changes in the valence band structure of $CsPbBr_3$ with the doping of Bi [9]. In the perfect $CsPbBr_3$ and the $CsPbBr_3$ with Bi_{Pb} defects, the states on the conduction band are mainly contributed by Pb atoms. However, when Bi atoms in the interstices of $CsPbBr_3$, the occupied state of the CBM changes from Pb states to Bi states as shown in the figure 4(c). Although the effect of these defects on the band gap is very weak, Bi_i defects directly change the electronic distribution of $CsPbBr_3$. Raihana *et al* observed that Bi doping promoted charge transfer in $CsPbBr_3$ [8]. We speculate that Bi_i defect may be the cause of promoting charge transfer. Because Bi_i defects as bridges connect more Br atoms, which is also easier to accept the electrons of Br atoms.

4. Conclusion

Three issues are highlighted in this article: What defects are induced by Bi doping? What is the cause of red-shift? Will Bi impurities cause changes in band structure of $CsPbBr_3$? The calculation of defect formation energy shows that Bi_{Pb} and Bi_i defects are stable. Then the mechanism of how defects lead to red-shift phenomenon is studied. There are two reasons. 1. The transition donor levels induced by Bi_{Pb} and Bi_i defects are slightly lower than CBM of $CsPbBr_3$. Thus the electrons can be excited with absorbing <2.36 eV energy, which eventually leads to the red shift of the absorption spectrum. 2. The Bi_i and Bi_{pb} also cause small changes in $CsPbBr_3$ lattice, resulting in the decrease of band gaps of 0.08 and 0.11 eV. The values of red shift induced by Bi_{Pb} and Bi_i defects were also estimated to be 150 meV and 270 meV respectively, which are close to the experimental red shifts of 140 meV. Finally, the effect of defects on the electronic structure is discussed. Olga *et al's* conclusion is confirmed that Bi doping does not affect the electron distribution of valence bands. According to the calculation, different defects will change the electron distribution of the conduction bands. The Bi_{Pb} does not affect the electron distribution of conduction bands. However, Bi_i defects change the electron distribution of the conduction band. For the system including Bi_i defects, we observed an obvious Bi atomic peak at the edge of the conduction band from the density-of-states diagram. We speculated that Bi_i defect may be the cause of promoting charge transfer as reported by Raihana Begum *et al*. Because Bi_i defects as bridges do connect many Br atoms, which is also easier to accept the electrons of Br atoms.

Acknowledgments

The authors thank the Changsha Supercomputer Center for computation. This work was supported by the National Natural Science Foundation of China (No. 51972103, 21938002), the Key Projects of Hunan Provincial Science and Technology Plan (No. 2017GK2231), and the Hunan Provincial Innovation Foundation for Postgraduate (No. CX2018B161).

Conflicts of interest

There are no conflicts of interest to declare.

ORCID iDs

Jun-Liang Yang https://orcid.org/0000-0002-5553-0186
Meng-Qiu Cai https://orcid.org/0000-0002-5364-725X

References

[1] Zhiping W, Qianqian L, Bernard W, Greyson C M, Yen-Hung L, Matthew T K, Michael B J, Laura M H and Henry J S 2018 *Nat. Energy* **3** 855–61
[2] Yu C *et al* 2018 *Nature* **562** 249–53
[3] Kebin L *et al* 2018 *Nature* **562** 245–8
[4] Xiangtong Z, Hua W, Yue H, Yixian P, Shixun W, Zhifeng S, Vicki L C, Shengnian W, Yu Z and William W Y 2019 *J. Phys. Chem. Lett.* **10** 1750–6
[5] Qingsong H, Zha L, Zhifang Tan, Huaibing S, Cong G, Guangda N, Jiantao H and Jiang T 2018 *Nanocrystals. Adv. Opt. Mater.* **6** 1700864
[6] Anu B and Vijay K 2019 *J. Phys. Chem.* C **123** 6965–9
[7] Yang Z, Jie C, Osman M B and Hong-Tao S 2018 *Chem. Mater.* **30** 6589–613
[8] Raihana B, Manas R P, Ahmed L A, Banavoth M, Noktan M A, Ghada H A, Mohamed N H, Osman M B and Omar F M 2017 *J. Am. Chem. Soc.* **139** 731–7
[9] Olga A L, Anna A M, Vladimir V S, Yury V K, Vladimir K R, Alexei V E and Tsutomu M 2018 *J. Phys. Chem. Lett.* **9** 5408–11
[10] Kresse G 1996 *Phys. Rev.* B **54** 11169–86
[11] Blöchl P E 1994 *Phys. Rev.* B **50** 17953–79
[12] Junyu Z, Jie S, Zhenhua L, Mengyu L, Jingjing C and Yue H 2019 *Appl. Phys. Lett.* **114** 181902
[13] Biao L, Mengqiu L, Mengqiu C, Liming D and Junliang Y 2019 *Nano Energy* **59** 715–20
[14] Jian X, Jian-Bo L, Bai-Xin L and Bing H 2017 *J. Phys. Chem. Lett.* **8** 4391–6
[15] Cai K, Lv S Y, Song L N, Chen L, He J, Chen P, Au C T and Yin S F 2019 *J. Solid State Chem.* **269** 145–6
[16] Amirali A 2019 *Physica* E **108** 34–43
[17] Chen P, Meng L H, Chen L, Au C T and Yin S F 2019 *ACS Sustain. Chem. Eng.* **7** 14203–9
[18] Amirali A and Jaber J S 2019 *Appl. Surf. Sci.* **469** 781–91
[19] Tang J, Gao B, Pan J, Chen L, Zhao Z, Shen S, Guo J K, Au C T and Yin S F 2019 *Appl. Catal. A-Gen.* **558** 117281
[20] Zhao Y Q, Ma Q L, Liu B, Yu Z L and Cai M Q 2018 *Phys. Chem. Chem. Phys.* **20** 14718
[21] Zhao Y Q, Ma Q R, Liu B, Yu Z L, Yang J L and Cai M Q 2018 *Nanoscale* **10** 8677
[22] Zhao Y Q, Wang X, Liu B, Yu Z L, He P B, Wan Q, Cai M Q and Yu H L 2018 *Org. Electron.* **53** 50
[23] Yu Z L, Ma Q R, Liu B, Zhao Y Q, Wang L Z, Zhou H and Cai M Q 2017 *J. Phys. D: Appl. Phys.* **50** 465101
[24] Deng X Z, Zhao Q Q, Zhao Y Q and Cai M Q 2019 *Curr. Appl. Phys.* **19** 279
[25] Liu B, Long M Q, Cai M Q and Yang J L 2018 *J. Phys. D: Appl. Phys.* **51** 105101
[26] Zhang J R, Zhao Y Q, Chen L, Yin S F and Cai M Q 2019 *Appl. Surf. Sci.* **469** 27

[27] Ding Y F, Zhao Q Q, Yu Z L, Zhao Y Q, Liu B, He P B, Zhou H, Li K L, Yin S F and Cai M Q 2019 *J. Mater. Chem.* C **7** 7433–41
[28] Wu L J, Zhao Y Q, Chen C W, Wang L Z, Liu B and Cai M Q 2016 *Chin. Phys.* B **25** 107202
[29] Liu B, Wu L J, Zhao Y Q, Wang L Z and Cai M Q 2016 *Eur. Phys. J.* B **89** 80
[30] Cao D, Liu B, Yu H L, Hu W Y and Cai M Q 2015 *Eur. Phys. J.* B **88** 75
[31] Cao D, Liu B, Yu H L, Hu W Y and Cai M Q 2013 *Eur. Phys. J.* B **86** 504
[32] Cai M Q, Du Y and Huang B Y 2011 *Appl. Phys. Lett.* **98** 102907
[33] Cao D, Cai M Q, Hu W Y, Peng J, Zheng Y and Huang H T 2011 *Appl. Phys. Lett.* **98** 031910
[34] Cao D, Cai M Q, Hu W Y and Xu C M 2011 *J. Appl. Phys.* **109** 114107
[35] Liu B, Wu L J, Zhao Y Q, Wang L Z and Cai M Q 2016 *J. Magn. Magn. Mater.* **420** 218
[36] Cao D, Wang N, Wang J F, Zhou Y, Jiao Z W, Cai M Q and Hu W Y 2017 *Eur. Phys. J.* B **90** 188
[37] Yang D J, Du Y H, Zhao Y Q, Yu Z L and Cai M Q 2019 *Phys. Status Solidi* b **256** 1800540
[38] Liao C S, Zhao Q Q, Zhao Y Q, Yu Z L, Zhou H, He P B, Yang J L and Cai M Q 2019 *J. Phys. Chem. Solids* **135** 109060
[39] Deng X Z, Zhang J R, Zhao Y Q, Yu Z L, Yang J L and Cai M Q 2020 *J. Phys.:Condens. Matter.* **32** 065004
[40] Pan L Y, Ding Y F, Yu Z L, Wan Q, Liu B, and Cai M Q 2020 *J. Power Sources* **451** 227732
[41] Tang C H, Lu X M, Huang F Z, Cai M Q, Kan Y, Wang X F, Zhang C and Zhu J S 2011 *Solid State Commun.* **151** 280
[42] Lin S P, Zheng Y, Cai M Q and Wang B 2010 *Appl. Phys. Lett.* **96** 232904
[43] Yu H L, Wu Y Z, Jiang X F, Cai M Q, Gu L P and Yang G W 2013 *J. Appl. Phys.* **114** 173502
[44] Liu B, Long M Q, Cai M Q and Yang J L 2018 *Appl. Phys. Lett.* **112** 043901
[45] Yu Z L, Zhao Y Q, He P B, Liu B, Yang J L and Cai M Q 2020 *J. Phys.:Condens. Matter* **32** 065002
[46] Cao D, Cai M Q, Tang C H, Yu P, Hu W Y, Du Y, Huang B Y and Deng H Q 2010 *Eur. Phys. J.* B **74** 447–4
[47] Yu Z L, Zhao Y Q, Liu B, Yang J L and Cai M Q 2020 *J. Phys.:Condens. Matter* **32** 115703
[48] Tang L P, Li Q Z, Zhang C X, Ning F, Zhou W X, Tang L M and Chen K Q 2019 *J. Magn. Magn. Mater.* **488** 165354
[49] Zhang C X, Li Q Z, Tang L M, Yangke K K, Xiao J, Chen K Q and Deng H X 2019 *J. Mater. Chem.* C **7** 6052–7
[50] Peng Y Y, Du B Y, Xu X W, Yang J L, Lin J and Ma C Q 2019 *Appl. Phys. Express* **12** 066503
[51] Xia H Y, Tong X C, Zhang C J, Wang C H, Sun J, He J, Zhang J, Gao Y L and Yang J L 2018 *Appl. Phys. Lett.* **112** 233301
[52] Peng Y Y, Xiao S G, Yang J L, Lin J, Yuan W, Gu W B, Wu X Z and Cui Z 2017 *Appl. Phys. Lett.* **110** 261904
[53] Zewen X, Weiwei M, Jianbo W, David B M and Yanfa Y 2017 *Mater. Horiz.* **4** 206–16
[54] Zewen X, Weiwei M, Jianbo W and Yanfa Y 2016 *Phys. Chem. Chem. Phys.* **18** 25786–90
[55] Tingting S, Wan-Jian Y, Feng H, Kai Z and Yanfa Y 2015 *Appl. Phys. Lett.* **106** 103902
[56] Liu B, Wu L J, Wang L Z and Cai M Q 2016 *RSC Adv.* **6** 92473–8
[57] Wenmei M, Dongwen Y, Tianshu L, Lijun Z and Mao-Hua D 2018 *Adv. Sci.* **5** 1700662
[58] Zewen X and Yanfa Y 2017 *Adv. Energy Mater.* **7** 1701136